Self-Assembly of Two- and Three-Dimensional Particle Arrays by Manipulating the Hydrophobicity of Silica Nanospheres

Wei Wang* and Baohua Gu

Environmental Sciences Division, Oak Ridge National Laboratory, P.O. Box 2008, Oak Ridge, Tennessee 37831

Received: July 6, 2005; In Final Form: September 28, 2005

The surface hydrophobicity of colloidal silica (SiO_2) nanospheres is manipulated by a chemical graft of alkyl chains with silane coupling agents or by physical adsorption of a cationic surfactant. The surface-modified SiO_2 spheres can be transferred from the aqueous phase to organic solvents and readily self-assemble at the water−air interface to form two-dimensional (2D) particle arrays. Closely packed particle monolayers are obtained by adjusting the hydrophilic/hydrophobic balance of the synthesized SiO_2 spheres and may further be transferred onto solid substrates layer by layer to form three-dimensional (3D) ordered particle arrays with a hexagonal close-packed (hcp) crystalline structure. The 2D monolayer and 3D multilayer SiO_2 films exhibit photonic crystal properties, which were determined by the UV−visible spectroscopic analysis in transmission mode. In the multilayer films, the Bragg diffraction maxima increased with an increase in thickness of the particle layers. The experimentally observed diffraction positions are in good agreement with those that were theoretically calculated.

Introduction

Two- and three-dimensionally ordered structures or arrays of monodispersed colloidal spheres have attracted a great deal of attention[1] because of their important applications in fabricating colloidal photonic crystals with incomplete or complete photonic band gaps in designed ranges of frequencies.[2,3] The interest of these ordered particle arrays lie in the fact that it is possible to induce them to coalesce in a close-packed structure, which diffracts light in UV, visible, and near-infrared regions[4−7] in an manner analogous to the diffraction of X-rays from ordinary mineral crystals. The 3D particle arrays can be prepared by sedimentation and assembly at various controlled conditions; techniques include gravity sedimentation,[8,9] sedimentation on a template surface,[10,11] solvent evaporation[12] and depletion,[13] and assembly at a vertical wall.[14,15] For fabrication of 2D particle arrays, the most commonly used methods are self-assembly at the water−air interface[16,17] and the Langmuir−Blodgett (LB) technique,[18−24] although several other techniques, such as drop casting, spin coating, and field-enhanced or molecular-interaction-induced deposition, were also used. When the LB technique is employed to assemble the particle film, the particle ordering in the film was found to be strongly dependent on the particle hydrophobicity.[14−24] In this work, we present methods for transferring hydrophilic SiO_2 colloids into organic solvents and demonstrate that 2D and 3D colloidal crystals can be readily fabricated via self-assembly of hydrophobic SiO_2 colloids at the water−air interface.

Experimental Procedure

Materials. Tetraethyl orthosilicate (TEOS, ≥99%) and $NH_3 \cdot H_2O$ (29.4%) were obtained from Fluka and J. T. Baker, respectively. Dodecyltriethoxysilane (DTEOS), *n*-octadecyltrimethoxysilane (95%, OTMOS), phenyltriethoxysilane (PTEOS), and *p*-tolyltrimethoxysilane (TTMOS) were obtained from Gelest, Inc. Absolute ethanol, chloroform, and cyclohexane came from GE Science. All chemicals were used as received. Deionized water with a resistivity of >18.0 MΩ·cm was obtained from a Millipore-Q Plus water purifier and used throughout the experiment.

Synthesis of Silica Colloids. Monodispersed SiO_2 nanoparticles were synthesized by hydrolysis of TEOS in an alcohol medium in the presence of water and ammonia by a modified procedure originally described by Stöber et al.[25] Detailed descriptions of synthesizing these spherical SiO_2 nanoparticles with controlled sizes in the range of 100 to 800 nm have been presented elsewhere.[7,17]

Colloidal Surface Modification and Phase Transfer. The hydrophilic nature of SiO_2 colloids makes it difficult to disperse or transfer pure SiO_2 nanoparticles into organic solvents. Therefore, the synthesized SiO_2 spheres were surface modified to become hydrophobic. Two different techniques were used for the surface modifications.

First, after completion of the TEOS hydrolysis, 10 mL of CH_2Cl_2 solution containing 1−10 vol % silane agent (OTMOS, DTEOS, PTEOS, and TTMOS) was added dropwise into an ∼250 mL reaction mixture containing ∼5 g of SiO_2, and the reaction was allowed to continue for a period of 12 h. The degree of surface hydrophobicity of SiO_2 spheres was controlled by the amount of the silane agent used, ranging from 0.1 to 1 silane molecule per square nanometer of the silica sphere surfaces. The specific surface area of silica spheres was calculated based on an average particle size obtained from transmission electron microscope (TEM) images. Upon completion of the reaction, the surface-modified silica colloids were separated and collected by centrifugation, and are readily redispersed into organic solvents such as chloroform and cyclohexane. Water-soluble impurities, if any, can be removed by repeated washing with deionized water.

In the second technique, synthesized silica colloids were separated and cleaned first by an ethanol wash, followed by

* Address correspondence to this author. E-mail: wangw@ornl.gov.

10.1021/jp053692s CCC: $30.25
Published on Web 11/04/2005

three water washes. The washed SiO_2 nanoparticles were redispersed into an aqueous CTAB surfactant solution at a concentration of 5×10^{-3} M. The reactant mixture was stirred for 2 h to allow sorption of CTAB onto silica. This was followed by the addition of an organic solvent (100 mL) such as chloroform and cyclohexane and 0.5 g of NaCl under vigorous stirring for about 10 min. The CTAB-modified silica nanoparticles were thus transferred into the organic phase; they were washed repeatedly with deionized water to remove excess free CTAB molecules.

Measurements. The particle sizes and polydispersity of the silica nanoparticles were examined by dynamic light scattering (DLS) measurements, using a Brookhaven 90Plus/ZetaPlus instrument.

Scanning electron microscope (SEM) images of silica spheres were taken with a Hitachi S-4700 electron microscope at 5 or 15 kV. Particles were deposited on a glass slide and coated with platinum before SEM analysis.

Direct imaging of silica nanoparticles also was observed by a Hitachi F 2000 TEM under an acceleration voltage of 200 kV. Particle film was transferred onto a Formvar/carbon film supported by a 300 mesh copper grid (Ted Pella Ltd.), and the solvent was allowed to evaporate to dryness before analysis.

Optical transmission spectra were obtained with use of a HP 8453 spectrophotometer with an integration time of 5 s. The Fourier transform infrared spectroscopy (FTIR) spectra of dried particles were recorded in diffusion reflectance mode with a Nicolet Magna-IR760 spectrometer. Raman spectra of dried particles were taken with a Renishaw spectrometer equipped with a Leico microscope and a 785-nm diode laser.

Results and Discussion

Surface Modification of Silica Nanoparticles. Monodispersed SiO_2 colloid particles were synthesized with use of the classical Stöber technique by the hydrolysis of TEOS (eqs 1−3):

$$\equiv Si-OC_2H_5 + H_2O \rightarrow \equiv Si-OH + C_2H_5OH \quad (1)$$

$$\equiv Si-OC_2H_5 + \equiv Si-OH \rightarrow \equiv Si-O-S\equiv + C_2H_5OH \quad (2)$$

$$\equiv Si-OH + \equiv Si-OH \rightarrow \equiv Si-O-Si\equiv + H_2O \quad (3)$$

After completion of the above reactions, a second silane agent with hydrophobic alkyl tails was introduced (eq 4) and anticipated to form a hydrophobic layer or a monolayer (theoretically) on the SiO_2 surface:

$$\equiv Si-OH + (R^IO)_3-Si-R^{II} \rightarrow \equiv Si-O-Si-R^{II} + ROH \quad (4)$$

where R^I is an alkyl group of $-CH_3$ or $-C_2H_5$, and R^{II} is octadecyl ($-C_{18}H_{37}$), dodecyl ($-C_{12}H_{23}$), phenyl ($-C_6H_5$), or tolyl ($-C_7H_7$). The presence of this hydrophobic alkyl layer on silica surfaces was confirmed by the FTIR analysis of dried SiO_2 nanoparticles before and after surface modification with OTMOS (Figure 1). The C−H stretching bands of alkyl chains at 2925 and 2852 cm^{-1} were clearly observed in SiO_2 nanoparticles modified with OTMOS. Also, the graft of alkyl chains affects surface structure, as indicated by the red-shift of the surface silanol O−H stretching band from ~3623 cm^{-1} to ~3398 cm^{-1}. This spectral shift suggests that the H-bonding weakened remarkably after the surface modification.[26]

The surface-modified silica nanocolloids became hydrophobic and thus could readily be transferred or dispersed into organic solvents. Since only a small amount of silane coupling agent was used for the surface modification, no new silica spheres or nuclei were formed, and no changes in particle sizes and size distribution were observed in TEM and SEM images.

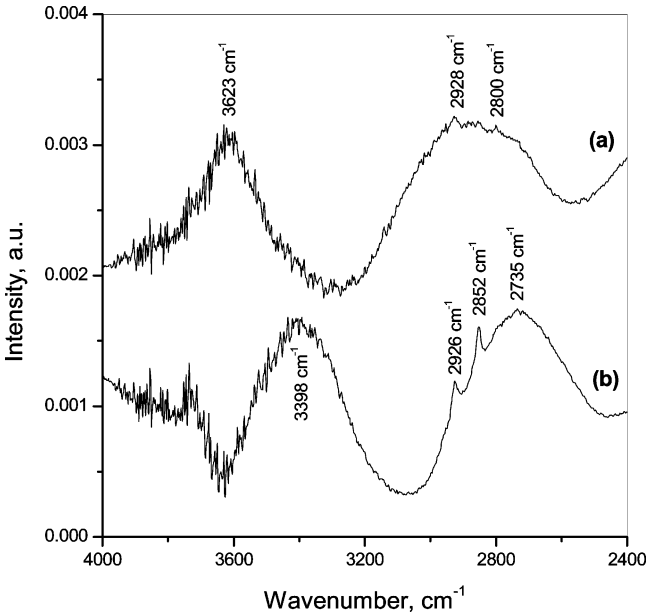

Figure 1. Diffuse reflectance FTIR spectra of dried SiO_2 nanoparticles (a) before and (b) after surface modification with OTMOS.

In addition to the use of these silane coupling agents for surface modification, the cationic surfactant CTAB also is known to be strongly sorbed by SiO_2 and was examined for the modification of SiO_2 surfaces.[27,28] In the presence of a low concentration of NaCl as an inducer, the CTAB-capped SiO_2 nanoparticles became hydrophobic and could thus migrate from the aqueous phase into an organic solvent. A CTAB concentration of 5×10^{-3} M was used for this transfer process. This concentration is crucial because if the CTAB concentration is too low, insufficient adsorption of CTAB occurs on the SiO_2 surface; silica particles may aggregate at the water−organic solvent interface and give low particle transfer efficiency. On the other hand, if the CTAB concentration is too high, the particle transfer efficiency also became low because of the formation of CTAB micelles, which increase the colloidal stability of SiO_2 particles in the aqueous phase. In the aqueous phase, CATB molecules can also form bilayers or multilayers on a SiO_2 surface by physical adsorption. The addition of inorganic salts was to break the bilayer or the multilayer so that only a monolayer of CTAB could be sorbed by the electrostatic interaction with its alkyl tails pointing to the aqueous phase and thus make the particle surface hydrophobic. The remains of CTAB on hydrophobic SiO_2 surface were confirmed by the presence of Raman spectral bands (Figure 2) for adsorbed CTAB on SiO_2 nanoparticles, including the N−H stretching mode at 3042 cm^{-1}, the CH_3 stretching mode at 2932 cm^{-1}, the CH_2 stretching mode at 2855 cm^{-1}, the CH_2 scissoring mode at 1450 cm^{-1}, the CH_2 twisting mode at 1302 cm^{-1}, and the symmetric $H_2C-N^+-(CH_3)_3$ mode at 759 cm^{-1}.

Preparation of Ordered 2D Arrays. One of the major applications for hydrophobic silica nanocolloids is in the preparation of 2D particle arrays. Here we report the fabrication of 2D arrays by self-assembly of hydrophobic SiO_2 nanoparticles at the water−air interface. Experimentally, the surface-modified hydrophobic SiO_2 nanoparticles were first dispersed in a nonpolar solvent, such as chloroform or cyclohexane. The suspension was then spread on the water surface. As the solvent evaporates, SiO_2 nanoparticles self-assembled into a 2D film

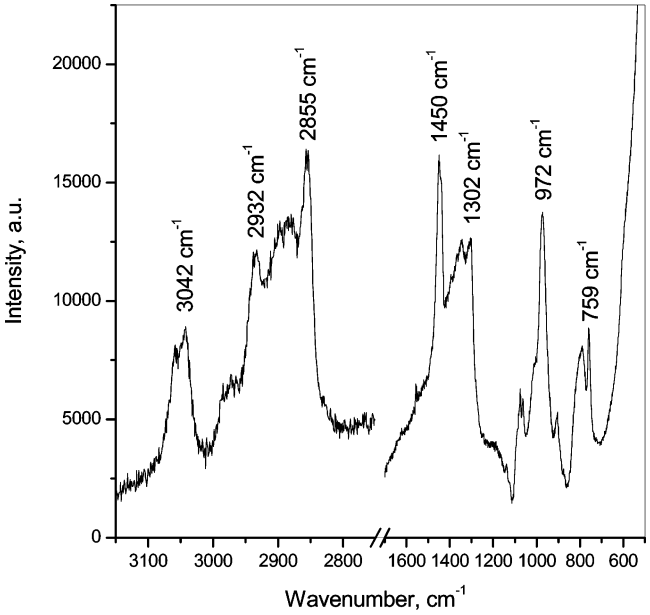

Figure 2. Raman spectra of CTAB-capped SiO_2 nanoparticles. Particles were dried on a quartz plate from its chloroform suspension.

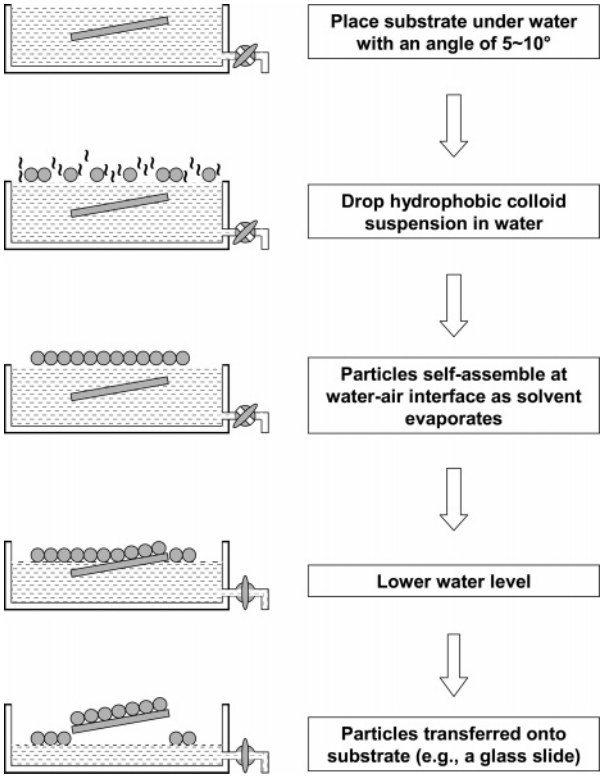

Figure 3. Schematic illustration of the transfer of a self-assembled nanoparticle monolayer onto a solid substrate from the water surface.

or 2D arrays due to the thermodynamic balance between the interfacial tensions at the particle−air and the particle−water interfaces. This 2D nanoparticle film could then be transferred onto a solid substrate (such as a glass slide), as schematically illustrated in Figure 3.

Figure 4 shows SEM images of SiO_2 2D arrays deposited on glass slides. Two different OTMOS concentrations were used for the modification of silica surfaces, and the calculated OTMOS sorption was about 1 and 0.2 molecules per square nanometer, respectively. The amount of sorbed OTMOS silane agent played a crucial role in controlling particle self-assembly processes and therefore the hydrophobocity of silica particles.

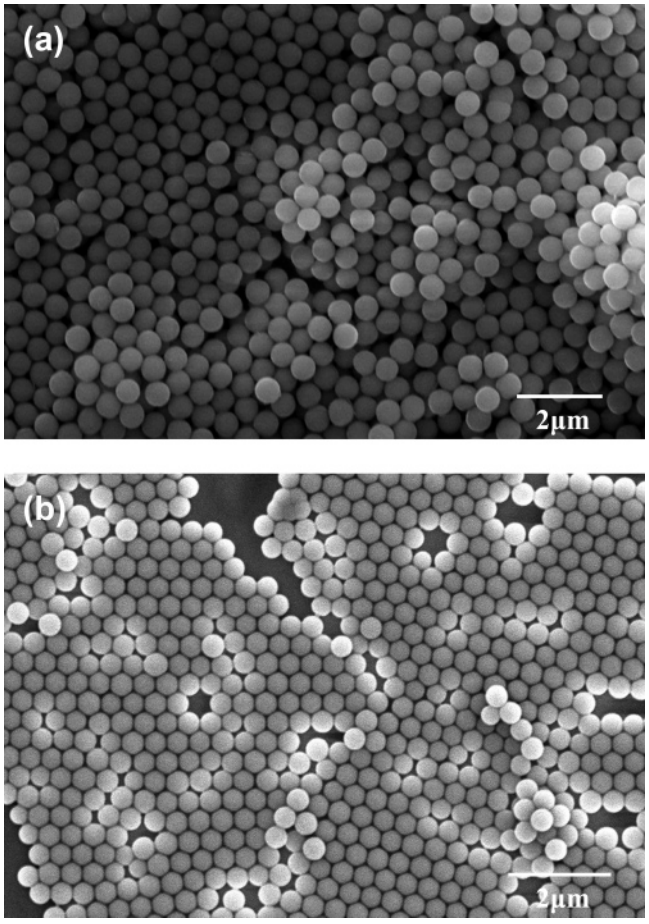

Figure 4. SEM images of self-assembled SiO_2 colloidal particle arrays on glass slides. SiO_2 particle surfaces were modified with OTMOS at initial concentrations of (a) 1 silane molecule per nm^2 and (b) 0.2 silane molecules per nm^2.

The image in Figure 4a shows some disordered particle islands, which were likely formed due to the use of a relatively high surface coverage of OTMOS (1 molecule per square nanometer). Strong hydrophobic interaction between the octadecyl alkyl chains may have resulted in the particle agglomeration and the formation of disordered particle multilayers. To reduce the hydrophobicity of the modified SiO_2 spheres, a reduced amount of OTMOS could be used for the surface modification of SiO_2 partilces. However, particles may simply disperse into the water when an insufficient amount of OTOMS is used and grafted onto silica surfaces so that they remain hydrophilic. We found that SiO_2 colloids modified with OTMOS in the amount of 0.2 molecule per square nanometer formed a relatively homogeneous particle monolayer (Figure 4b). It is therefore essential to attain a proper hydrophilic/hydrophobic balance on the surface of particles. The hydrophobicity of silica particles also may be controlled by using different silane agents with different alkyl chains, such as DTEOS and PTEOS, which are less hydrophobic (Figure 5).

The CTAB-modified SiO_2 particles also self-assemble into a close-packed monolayer at the water−air interface. Previous studies have used mixed CTAB and SiO_2 to form 2D SiO_2 particle arrays directly at the water−air interface,[19,21] and these particle arrays showed a decreased particle ordering at high CTAB concentration. In our method, we suspended CTAB capped SiO_2 nanoparticles in chloroform, and 2D particle arrays were prepared by self-assembling hydrophobic silica particles at the water−air interface, as described earlier (Figure 6). Highly ordered silica arrays thus obtained although the particle arrays

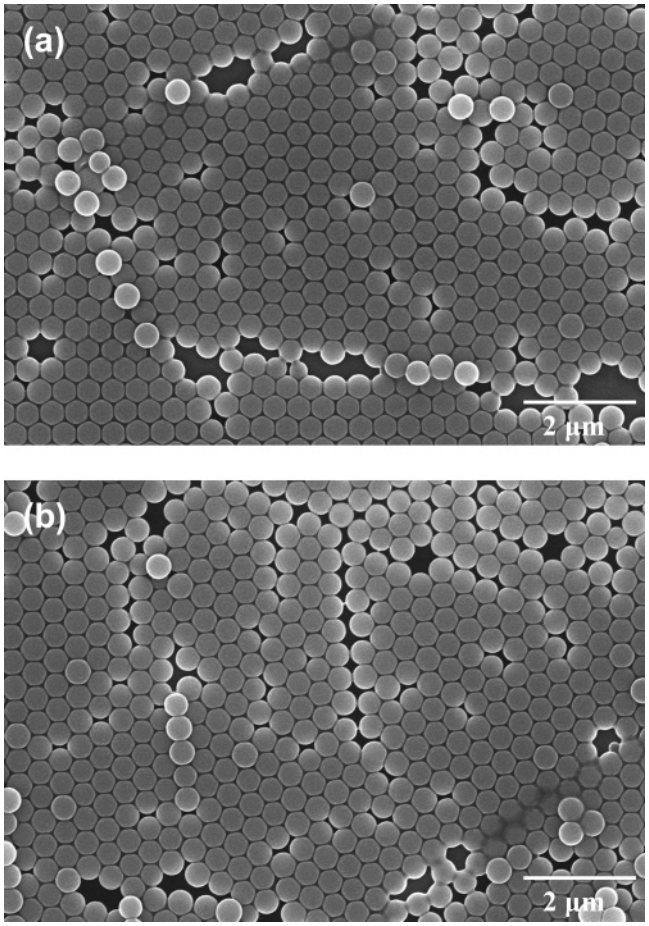

Figure 5. SEM images of self-assembled SiO_2 particle ($D = 440$ nm) arrays on glass slides. SiO_2 particle surfaces were modified with (a) DTEOS at the initial concentration of 0.3 silane molecules per nm^2 surface and (b) PTEOS at the initial concentration of 0.4 silane molecules per nm^2 surface.

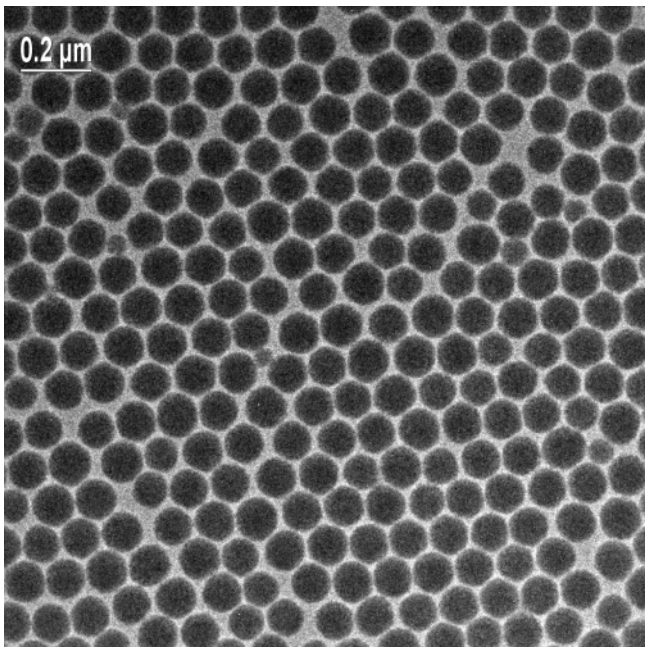

Figure 6. TEM image of a monolayer of SiO_2 colloid particle ($D = 110$ nm) array transferred onto a TEM grid. SiO_2 particle surfaces were modified with CTAB.

showed a less compact structure in comparison with those of OTMOS-, DTEOS-, PTEOS-, and TTMOS-modified particle arrays. Note that the CTAB-modified SiO_2 colloidal suspension must be washed thoroughly with water because excess CTAB molecules in organic solvents may form multilayers on SiO_2 spheres so as to reduce the uniformity of particle hydrophobicity and thus particle ordering in the 2D arrays at the water−air interface.

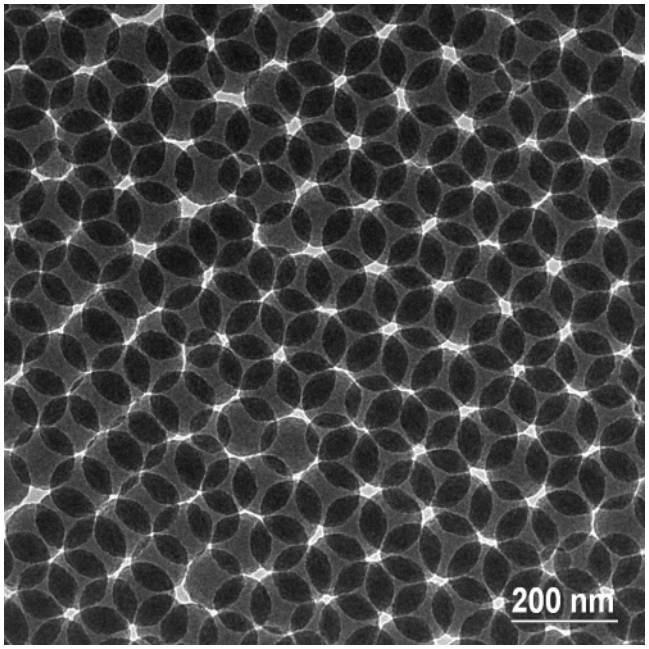

Figure 7. TEM image of a two-layer SiO_2 colloid particle ($D = 110$ nm) array transferred onto a TEM grid. SiO_2 particle surfaces were modified by CTAB.

Ordered 3D Particle Arrays. Three-dimensional colloidal particle arrays are of particular interest because 3D periodic structures possessing photonic band gaps in every direction are suitable for directing photons. These 3D crystalline multilayer photonic crystals may be prepared layer by layer by using solvent evaporation[29−32] and LB[33−35] methods. We found that the self-assembled monolayer of silica 2D particle arrays at the water−air interface also could be transferred onto the solid substrate layer by layer to form ordered 3D multilayer particle arrays using the process described in Figure 3. This is illustrated in a TEM image of the two-layer particle arrays (Figure 7), which clearly show a hexagonal closely packed (hcp) structure of assembled SiO_2 spheres ($D = 110$ nm). These highly ordered colloidal particle arrays diffract light in UV and visible ranges depending on particle sizes. For example, the Bragg diffraction was observed at 253 nm with normal light incidence to the colloid film for CTAB-modified 110-nm SiO_2 particles, and its intensity increased with an increase in the colloid film thickness (Figure 8). With decreasing incident light angles to the colloid film, its diffraction peak position also shifted to lower wavelengths (inset in Figure 8), exhibiting the typical characteristics of a photonic crystal structure. With increasing particle sizes and increased distance between particles, the diffraction peaks were found to shift from UV to visible and near-IR regions. For example, we observed diffraction at 503 nm for a colloid film of OTMOS-modified 440-nm SiO_2 particles (Figure 9). This diffraction peak was likely from secondary diffraction of the colloidal arrays because the first-order diffraction should have shifted to the near-IR region. These diffraction patterns approximately obey Bragg's equation:

$$m\lambda = 2n_{\text{eff}}d \sin\theta \tag{5}$$

where m is the order of diffraction, λ is the diffracted wavelength

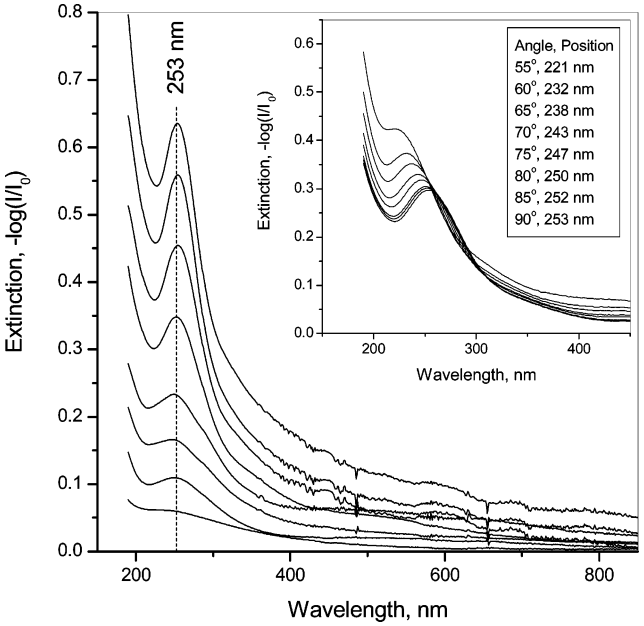

Figure 8. UV−visible transmission spectra of SiO_2 3D particle arrays on a quartz plate at normal light incidence. The particle size was 110 nm, and layer thickness was 1 to 8 (from bottom to top). Inset: Spectra at different angles of incident light to a colloid particle film with a thickness of 5 layers.

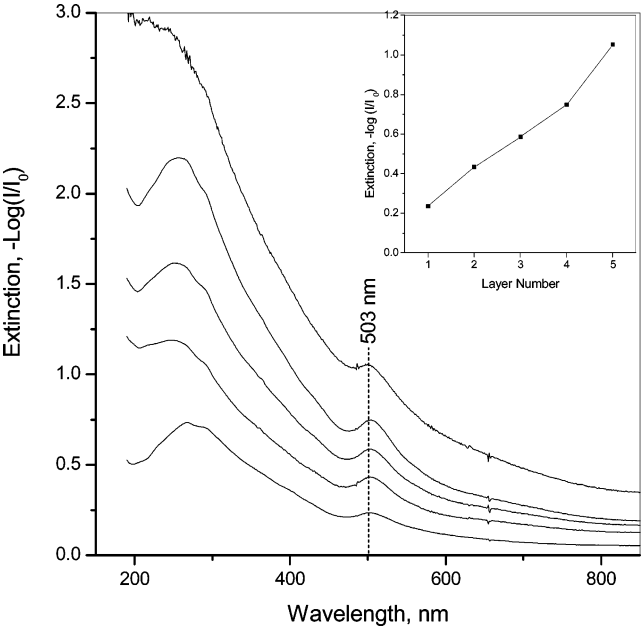

Figure 9. UV−visible transmission spectra of SiO_2 3D particle arrays on a quartz plate at normal light incidence with increasing particle layers from 1 to 5 (from bottom to top). The particle size was 440 nm. The inset shows the dependence of diffraction intensity at 503 nm on particle layer thicknesses.

in a vacuum, n_{eff} is the effective refractive index of the system (medium and colloidal particle), d is the spacing between the diffracting planes, and θ is the Bragg glancing angle between the incident light propagation direction and the diffracting plane. The n_{eff} can be calculated by assuming a volume fraction of 74% for closely packed SiO_2 colloid spheres in air and a refractive index of 1.445 for amorphous silica (eq 6).

$$n_{eff} = \varphi_{SiO_2} \cdot n_{SiO_2} + \varphi_{air} \cdot n_{air} = 0.74 \times 1.445 + 0.26 \times 1 = 1.3293 \quad (6)$$

For an hcp lattice, the diameter of the spheres, D, is related to the lattice parameter by $d = 0.866D$, and thus the first-order diffraction at normal light incidence is given as

$$\lambda_{max} = 2n_{eff} \cdot 0.866D \quad (7)$$

The calculated Bragg diffraction maximum at normal light incidence is therefore at 253 nm for the first-order diffraction of 110-nm SiO_2 particles and at 507 nm for the second-order diffraction of 440-nm SiO_2 particles, respectively. The calculated values agree well with the experimentally determined peak positions at 253 and 503 nm in UV−visible spectra (Figures 8 and 9). However, if assuming a fcc (face-centered cubic) lattice with $d = 0.816\ D$, there is 15−30 nm deviation between the calculated and measured Bragg diffraction maxima.

Conclusions

This paper has described methods for modifying the surface hydrophobicity of SiO_2 nanoparticles so that the modified SiO_2 spheres could be transferred from the aqueous phase to organic solvents to form 2D and 3D particles arrays. An adjustment of the hydrophilic/hydrophobic balance of the synthesized nanoparticles is achieved with silane coupling agents or cationic surfactants. The surface-modified hydrophobic nanoparticles readily self-assemble at the water−air interface to form 2D particle arrays. The monolayer could also be transferred onto solid substrates layer by layer to form 3D ordered particle arrays with the hcp crystalline structure. The 2D monolayer and 3D multilayer SiO_2 films showed photonic crystal properties, which were detected by transmission measurement in the UV−visible region. In the multilayer films, the Bragg diffraction maxima increased gradually with an increase in the particle layer thickness. The experimentally observed diffraction positions are in good agreement with those theoretically calculated.

Acknowledgment. This research was supported in part by the Office of Basic Energy Sciences, U.S. Department of Energy (DOE) and by Oak Ridge National Laboratory (ORNL) Directed Research and Development Funds. ORNL is managed by UT-Battelle, LLC, for U.S. Department of Energy under contract DE-AC05-00OR22725.

References and Notes

(1) Joannopoulos, J. D.; Meade, R. D.; Winn, J. N. *Photonic Crystals*: Princeton University Press: Princeton: NJ, 1995.
(2) Yablonovich, E. *Phys. Rev. Lett.* **1987**, *58*, 2059.
(3) John, S. *Phys. Rev. Lett.* **1987**, *58*, 2486.
(4) Xia, Y.; Gates, B.; Li, Z. Y. *Adv. Mater.* **2001**, *13*, 409.
(5) Asher, S. A.; Holtz, J.; Weissman, J.; Pan, G. S. *MRS Bull.* **1998**, *23*, 44.
(6) Velve, O. D.; Kaler, E. W. *Adv. Mater.* **2000**, *12*, 531.
(7) Wang, W.; Gu, B.; Liang, L.; Hamilton, W. A. *J. Phys. Chem. B* **2003**, *107*, 12113.
(8) Miguez, H.; Meseguer, F.; Lopez, C.; Blanco, A.; Moya, J. S.; Requena, J.; Mifsud, A.; Fornes, V. *Adv. Mater.* **1998**, *10*, 480.
(9) Vos, W. L.; Sprik, R.; van Blaaderen, A.; Imhof, A.; Lagendijk, A.; Wegdam, G. H. *Phys. Rev. B* **1996**, *53*, 16231.
(10) Yi, G.-R.; Moon, J. H.; Yang, S.-M. *Chem. Mater.* **2001**, *13*, 2613.
(11) Park, S. H.; Xia, Y. *Adv. Mater.* **1998**, *10*, 1045.
(12) Jiang, P.; Ostijic, G. N.; Narat, R.; Mittelman, D. M.; Colvin, V. L. *Adv. Mater.* **2001**, *13*, 389.
(13) Lu, Y.; Yin, Y.; Gates, B.; Xia, Y. *Langmuir* **2001**, *17*, 6344.
(14) Dimitrov, A. S.; Nagayama, K. *Langmuir* **1996**, *12*, 1303.
(15) de Hoog, E. H. A.; de Jong-van Steensel, L. I.; Snel, M. M. E.; van der Eerden, J. P. J. M.; Lekkerkerker, H. N. W. *Langmuir* **2001**, *17*, 5486.
(16) Yamaki, M.; Higo, J.; Nagayama, K. *Langmuir* **1995**, *11*, 2975.
(17) Wang, W.; Gu, B.; Liang, L. Y.; Hamilton, W. *J. Phys. Chem. B* **2003**, *107*, 3400.
(18) van Duffel, B.; Ras, R. H. A.; De Schryver, F. C.; Schoonheydt, R. A. *J. Mater. Chem.* **2001**, *11*, 3333.

(19) Szekeres, M.; Kamalin, O.; Schoonheydt, R. A.; Wostyn, K.; Clays, K.; Persoons, A.; Dékány, I. *J. Mater. Chem.* **2002**, *12*, 3268.

(20) Szekeres, M.; Kamalin, O.; Grobet, P. G.; Schoonheydt, R. A.; Wostyn, K.; Clays, K.; Persoons, A.; Dékány, I. *Colloids Surf. A* **2003**, *227*, 77.

(21) Reculusa, S.; Ravaine, S. *Chem. Mater.* **2003**, *15*, 598.

(22) Reculusa, S.; Massé, P.; Ravaine, S. *J. Colloid Interface Sci.* **2004**, *279*, 471.

(23) Bardosova, M.; Hodge, P.; Pach, L.; Pemble, M. E.; Smatko, V.; Tredgold, R. H.; Whitehead, D. *Thin Solid Films* **2003**, *437*, 276.

(24) Muramatsu, K.; Takahashi, M.; Tajima, K.; Kobayashi, K. *J. Colloid. Interface Sci.* **2001**, *242*, 127.

(25) Stöber, W.; Fink, A.; Bohn, E. *J. Colloid Interface Sci.* **1968**, *26*, 62.

(26) Pelmenschikov, A. G.; Morosi, G.; Gamba, A.; Zecchina, A.; Bordiga, S.; Paukshitis, E. A. *J. Phys. Chem.* **1993**, *97*, 11979.

(27) Wang, W.; Gu, B.; Liang, L.; Hamilton, W. A. *J. Phys. Chem. B* **2004**, *108*, 17477.

(28) Wang, W.; Gu, B.; Liang, L. *J. Dispersion Sci. Technol.* **2004**, *25*, 595.

(29) Duskhin, C. D. *Langmuir* **1993**, *9*, 3695.

(30) Denkov, D. N.; Velev, O. D.; Kralchevsky, P. A.; Ivanov, I. B.; Yoshimura, H.; Nagayama, K. *Langmuir* **1992**, *8*, 3183.

(31) Jiang, P.; Bertone, J. F.; Colvin, V. L. *Science* **2001**, *291*, 453.

(32) Yamasaki, T.; Tsutsui, T. *Jpn. J. Appl. Phys.* **1999**, *38*, 5916.

(33) Collier, C. P.; Saykally, R. J.; Shiang, J. J.; Henrich, S. E.; Heath, J. R. *Science* **1997**, *277*, 1978.

(34) Kurth, D. G.; Lechmann, P.; Lesser, C. *Chem. Commun.* **2000**, 949.

(35) Velikov, K. P.; Christova, C. G.; Dullens, R. P. A.; van Blaaderen, A. *Science* **2002**, *296*, 106.